JPE 4-4-3

A High-Performance Induction Motor Drive with 2DOF I-PD Model-Following Speed Controller

Fayez F. M. El-Sousy†

Electronics Research Institute (ERI)
Power Electronics & Energy Conversion Department, Cairo, Egypt

ABSTRACT

A robust controller that combines the merits of the feed-back, feed-forward and model-following control for induction motor drives utilizing field orientation control is designed in this paper. The proposed controller is a two-degrees-of-freedom (2DOF) integral plus proportional & rate feedback (I-PD) speed controller combined with a model-following (2DOF I-PD MFC) speed controller. A systematic mathematical procedure is derived to find the parameters of the 2DOF I-PD MFC speed controller according to certain specifications for the drive system. Initially, we start with the I-PD feed-back controller design, then we add the feed-forward controller. These two controllers combine to form the 2DOF I-PD speed controller. To realize high dynamic performance for disturbance rejection and set point tracking characterisitics, a MFC controller is designed and added to the 2DOF I-PD controller. This combination is called a 2DOF I-PD MFC speed controller. We then study the effect of the 2DOF I-PD MFC speed controller on the performance of the drive system under different operating conditions. A computer simulation is also run to demonstrate the effectiveness of the proposed controller. The results verify that the proposed 2DOF I-PD MFC controller is more accurate and more reliable in the presence of load disturbance and motor parameter variations than a 2DOF I-PD controller without a MFC. Also, the proposed controller grants rapid and accurate responses to the reference model, regardless of whether a load disturbance is imposed or the induction machine parameters vary.

Keywords: Indirect field orientation control, 2DOF I-PD controller, model following controllor (MFC), induction motor drive.

1. Introduction

Induction machines have many advantageous characteristics such as high robustness, reliability and low cost. Therefore, induction machine drives are used in high-performance industrial applications which require independent torque and speed control such as robotics, rolling mills, machine tools and tracking systems. They are based on complex, nonlinear, time-varying and temperature dependent mathematical models. To meet the requirements of high dynamic performance, field orientation control (FOC) is used to simplify and decouple the dynamic model of the induction machine. The FOC strategy is based upon the work of Hass and Blashke in

Manuscript received April 30, 2004; revised July. 16, 2004.
†Corresponding Author: : fayez@eri.sci.eg
Tel: +202-310554, Fax: +202-3351631, ERI

Germany thirty years ago. This technique improves the performance of an induction machine drive system to a level comparable to that of a DC machine. Therefore, FOC of induction machine drive systems has permitted high-performance dynamic responses using decoupled torque and flux control. In order to execute an indirect field orientation control (IFOC) strategy, current regulated pulse width modulated (CRPWM) inverters are usually employed to satisfy the current control requirements [1-4].

The use of conventional controllers to control field oriented machine drives has gained the widest acceptance in high-performance ac drive systems. However, conventional controllers have difficulty dealing with dynamic speed tracking, parameter variations and load disturbances. The dynamic performance of a field-oriented induction motor is affected by decoupling. For IFOC of an induction motor, the ideal decoupling between flux and torque will not be obtained if the nominal values of the rotor parameters used in the FOC are not tracked. The most important parameter to be considered is the rotor resistance. The adaptation of the FOC equation, ω_{sl}, is very important to achieve ideal decoupling. Various techniques have been reported to reduce the effects of rotor parameter variations on IFOC[5-8]. Several control techniques can be applied to induction motor drive systems to yield high performance. One of the most commonly used controllers in industrial applications is the proportional plus integral plus derivative (PID) controller. Other variations of PID controllers such as PI-D and I-PD controllers achieve the tracking and regulation characteristics as a result of their one-degree-of-freedom structure. Additionally, two-degrees-of-freedom (2DOF) IP or PI-D controllers which meet the tracking and regulation criteria for induction machines have been designed [9-14].

The author propose a hybrid controller for the speed control of the induction motor drive. It combines the advantages of the two-degrees-of-freedom (2DOF) and the model following control techniques. This IFOC induction motor drive system is composed of non-linear and linearized dynamic models of the induction motor in the general reference frame, the dynamic model of the IFOC technique (decoupling controller), d-q axes stator current controllers, speed controller, space vector PWM modulator and PWM inverter. The block schematic diagram of the IFOC induction machine drive system is shown in Fig. 1.

This paper presents quantitative analysis and design of the 2DOF I-PD MFC speed controller for a field oriented induction motor drive system. The controller is designed to achieve zero steady state error, minimum overshoot and minimum settling time, in other words, good dynamic response for disturbance rejection and set point tracking. The proposed 2DOF I-PD controller consists of an I-PD controller in the feed-back loop (also called integral plus proportional & rate feedback) and a feed-forward controller. To realize high dynamic performance for disturbance rejection and set point tracking characteristics, a model following controller (MFC) is designed and analyzed in addition to the 2DOF I-PD speed controller. A quantitative design procedure is derived to systematically find the parameters of the controller according to the given motor specifications. In addition to the tracking and regulation speed control specifications, the effects of the command change rate as well as the control effort are also considered in the proposed design procedure. To verify the design of the controller and the system performance, the drive system is simulated. The dynamic performance has been studied under load changes, taking into consideration the parameter variations of the induction machine. The simulation results are provided to demonstrate the effectiveness of the proposed controllers.

2. Dynamic Models of Induction Motor and Decoupling Controller (IFOC)

The state equation of the nonlinear dynamic *d-q* model of the induction machine at the arbitrary reference frame is expressed as follows [4].

$$\frac{d}{dt}\begin{bmatrix} i_{qs} \\ i_{ds} \end{bmatrix} = \begin{bmatrix} -k_{ss} & -\omega \\ \omega & -k_{ss} \end{bmatrix}\begin{bmatrix} i_{qs} \\ i_{ds} \end{bmatrix} + \begin{bmatrix} \frac{k_m}{\tau_r} & -k_m\omega_r \\ k_m\omega_r & \frac{k_m}{\tau_r} \end{bmatrix}\begin{bmatrix} \lambda_{qr} \\ \lambda_{dr} \end{bmatrix} + \frac{1}{\sigma L_s}\begin{bmatrix} V_{qs} \\ V_{ds} \end{bmatrix} \tag{1}$$

From (1-4), we can derive the perturbed model of the induction machine.

$$\frac{d}{dt}\begin{bmatrix}\lambda_{qr}\\ \lambda_{dr}\end{bmatrix}=\begin{bmatrix}\frac{L_m}{\tau_r} & 0\\ 0 & \frac{L_m}{\tau_r}\end{bmatrix}\begin{bmatrix}i_{qs}\\ i_{ds}\end{bmatrix}+\begin{bmatrix}-\frac{1}{\tau_r} & -(\omega-\omega_r)\\ (\omega-\omega_r) & -\frac{1}{\tau_r}\end{bmatrix}\begin{bmatrix}\lambda_{qr}\\ \lambda_{dr}\end{bmatrix} \tag{2}$$

$$\frac{d}{dt}\omega_r=-\frac{\beta}{J}\omega_r+\frac{(P/2)}{J}T_e-\frac{(P/2)}{J}T_L \tag{3}$$

$$T_e=\frac{3}{2}\cdot\frac{P}{2}\cdot\frac{L_m}{L_r}(\lambda_{dr}i_{qs}-\lambda_{qr}i_{ds}) \tag{4}$$

The IFOC dynamics for the induction machine (torque, slip angular frequency and voltage commands) can be derived from (1-4) respectively at $\lambda^e_{qr}\approx 0$ $d\lambda^e_{qr}/dt=0$, $d\lambda^e_{dr}/dt=0$ and $\omega=\omega_e$. The torque equation and slip angular frequency for rotor field orientation are given in (6-7) while the voltage commands of the indirect field orientation controller (IFOC) are given in (8-9).

$$\frac{d}{dt}\begin{bmatrix}\Delta i_{qs}\\ \Delta i_{ds}\\ \Delta\lambda_{qr}\\ \Delta\lambda_{dr}\\ \Delta\omega_r\end{bmatrix}=\begin{bmatrix}-k_{ss} & -\omega_o & \frac{k_m}{\tau_r} & -k_m\omega_{ro} & 0\\ \omega_o & -k_{ss} & k_m\omega_{ro} & \frac{k_m}{\tau_r} & 0\\ \frac{L_m}{\tau_r} & 0 & -\frac{1}{\tau_r} & -(\omega_o-\omega_{ro}) & 0\\ 0 & \frac{L_m}{\tau_r} & (\omega_o-\omega_{ro}) & -\frac{1}{\tau_r} & 0\\ K_{tj}\lambda^e_{dro} & -K_{tj}\lambda^e_{qro} & K_{tj}i^e_{dso} & -K_{tj}i^e_{qso} & -\frac{\beta}{J}\end{bmatrix}\begin{bmatrix}\Delta i_{qs}\\ \Delta i_{ds}\\ \Delta\lambda_{qr}\\ \Delta\lambda_{dr}\\ \Delta\omega_r\end{bmatrix}+\begin{bmatrix}\Delta V_{qs}/\sigma L_s\\ \Delta V_{ds}/\sigma L_s\\ \Delta V_{qr}/L_r\\ \Delta V_{dr}/L_r\\ -\Delta T_L K_j\end{bmatrix} \tag{5}$$

$$T_e=\frac{3}{2}\cdot\frac{P}{2}\cdot\frac{L_m^2}{L_r}i^{e*}_{ds}i^{e*}_{qs} \tag{6}$$

$$\omega_{sl}=\frac{1}{\tau_r}\cdot\frac{i^{e*}_{qs}}{i^{e*}_{ds}} \tag{7}$$

$$\begin{bmatrix}V^{e*}_{qs}\\ V^{e*}_{ds}\end{bmatrix}=\begin{bmatrix}R_s+L_s\sigma\frac{d}{dt} & \omega_e L_s\sigma\\ -\omega_e L_s\sigma & R_s+L_s\sigma\frac{d}{dt}\end{bmatrix}\begin{bmatrix}i^e_{qs}\\ i^e_{ds}\end{bmatrix}+\begin{bmatrix}e^e_{qs}\\ e^e_{ds}\end{bmatrix} \tag{8}$$

$$\begin{bmatrix}e^e_{qs}\\ e^e_{ds}\end{bmatrix}=\begin{bmatrix}\omega_e\lambda^e_{dr}\frac{L_m}{L_r}\\ 0\end{bmatrix} \tag{9}$$

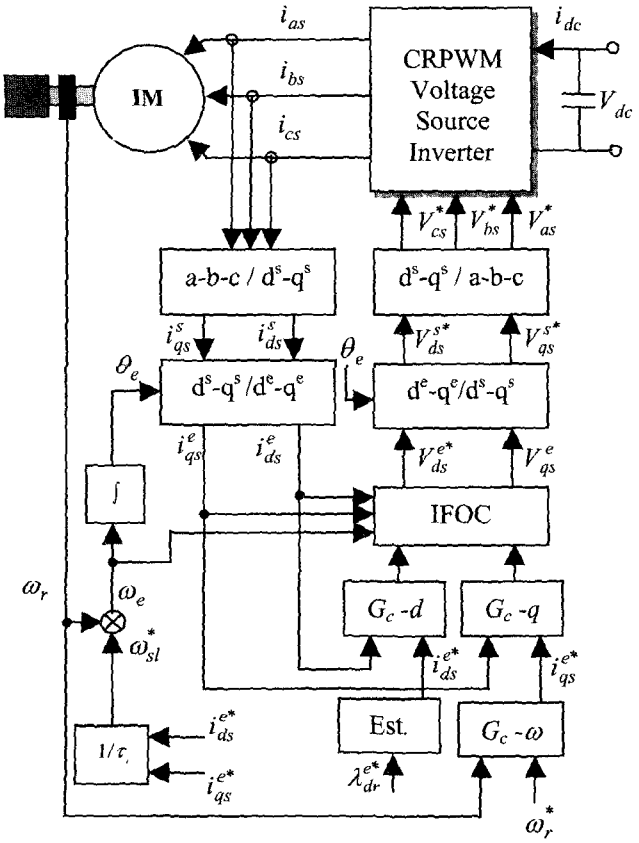

Fig. 1 Block schematic diagram of the IFOC induction motor drive system

where V_{qs}, V_{ds}, i_{qs} and i_{ds} are the stator voltages and currents, respectively. V_{qr}, V_{dr}, λ_{qr} and λ_{dr} are the rotor voltages and fluxes respectively. R_s, R_r, L_s and L_r are the resistance and self inductance of the stator and rotor respectively. L_m is the mutual inductance. ω_r, J and β are the electrical rotor speed, the effective inertia and the friction coefficient of the motor, respectively. T_e, T_L, τ_r, τ_s

and ω_{sl} are the electromagnetic torque, the load torque, the rotor time constant, the stator time constant and the slip angular frequency of the motor respectively. e_{qs}, e_{ds} ω and ω_e are the back *emfs*, the electrical angular frequency of the arbitrary reference frame and the electrical angular frequency of the synchronous reference frame respectively. σ and P are the leakage flux coefficient and the number of poles respectively. $\tau_r = L_r / R_r$, $\tau_s = L_s / R_s$, $\sigma = (L_s L_r - L_m^2) / L_s L_r$, $\tau_s^{'} = \sigma\tau_s$ $\tau_r^{'} = \sigma\tau_r$, $k_{ss} = (1/\sigma\tau_s + 1 - \sigma/\sigma\tau_r)$, $K_m = L_m / \sigma L_s L_r$ and $K_t = (3P/4).(L_m^2 / L_r).i_{ds}^{e*}$ are constants of the induction motor.

3. Design of the Proposed 2DOF I-PD Model-Following Speed Controller

In this section, the design procedures for the 2DOF I-PD MFC speed controller are developed. The current controllers have been designed in [4] and their configuration is known as proportional plus integral (PI) controllers. The closed loop transfer function of the q-axis current loop is given by:

$$G_i(s) = \frac{K_{pq}(s + K_{PI}^i)}{(s^2 + \tau_i s + K_{iq})} \tag{10}$$

3.1 2DOF I-PD Speed Controller

The controller consists of two parts, the I-PD controller in the feed-back loop and a feed-forward controller [15].

3.1.1 I-PD Feed-back Speed Controller

According to the block diagram shown in Fig. 2, the closed loop transfer function at $T_L(s) = 0$ is given by:

$$\frac{\omega_r(s)}{\omega_{rd}(s)} = \frac{K_{tmpq}(s + K_{PI}^i)}{s^4 + \tau_{3\omega}s^3 + \tau_{2\omega}s^2 + \tau_{1\omega}s + \tau_{\circ\omega}} \tag{11}$$

Using the performance index ITAE robust technique, we can determine the controller parameters.

$$\frac{C(s)}{R(s)} = \frac{\omega_n^4}{s^4 + 2.1\omega_n s^3 + 3.4\omega_n^2 s^2 + 2.7\omega_n^3 s + \omega_n^4} \tag{12}$$

From (11) and (12), the controller parameters can deduced as follows.

$$K_p^{\omega} = \frac{\left(2.7\omega_n^3 - K_{iq}/\tau_m - \omega_n^4 / K_{PI}^i\right)}{K_{tmpq} K_{PI}^i} \tag{13}$$

$$K_i^{\omega} = \frac{\omega_n^4}{K_{tmpq} K_{PI}^i} \tag{14}$$

$$K_d^{\omega} = \frac{\left(2.1\omega_n - \tau_i - 1/\tau_m\right)}{K_{tmpq}} \tag{15}$$

3.1.2 I-PD Feed-forward Speed Controller

According to the block diagram shown in Fig. 3, the closed loop transfer function at $T_L(s) = 0$ is given by:

$$\frac{\omega_r(s)}{\omega_{rd}(s)} = \frac{K_{tmpq}(s + K_{PI}^i)}{s^4 + \tau_{3\omega}s^3 + \tau_{2\omega}s^2 + \tau_{1\omega}s + \tau_{\circ\omega}} . G_{ff}(s) \tag{16}$$

Accordingly, we can obtain the feed-forward controller transfer function from (12 and 16) which has the following relation.

$$G_{ff}(s) = \frac{\omega_n^4}{K_{tmpq} K_i^{\omega} (s + K_{PI}^i)} \tag{19}$$

This relationship is known as a lag compensator. To improve the relative stability of the system, we add a lead part to this controller as follows.

$$\overline{G}_{ff}(s) = \overline{K} \frac{(1 + \tau_1 s)}{(1 + \tau_2 s)} \tag{20}$$

3.2 Model-Following Controller (MFC)

To increase the resistance of the field oriented induction motor drive to parameter variations and operating condition changes we added a model following controller (MFC) to the system. The MFC is designed to compensate the deviation between the desired tracking response trajectory and the actual drive system response. Taking into consideration the current control loops, the closed loop tracking transfer function of the I-PD controller used in the nominal model is obtained. and used as the desired tracking response trajectory of the drive

system given in (11). As shown in Fig. 4, a compensation control signal is obtained by taking the difference between the output of the MFC and the output of the drive system when regulated by another controller. This signal improves the load regulation response and tracking characteristics. The compensation control signal can be obtained from a proportional (P) controller or proportional plus integral (PI) controller. The design of the MFC with P-controller and PI-controller is as follows.

3.2.1 MFC with Proportional Controller (P-MFC)

The value of the gain of the P-MFC is based on the performance index ITAE robust technique. Taking into consideration the current control loop G_i *(s),* the closed loop transfer function of the drive system is obtained from Fig. 4.

$$G_{mfc}(s) = \frac{K_{tmpq}(s + K_{PI}^{i})}{s^4 + \tau_{3\omega}s^3 + \tau_{2\omega}s^2 + \tau_{1\omega}s + \tau_{\circ\omega}} \tag{21}$$

$$\frac{\omega_r(s)}{\omega_r^{mfc}(s)} = \frac{a_4s^4 + a_3s^3 + a_2s^2 + a_1s + a_\circ}{b_4s^4 + b_3s^3 + b_2s^2 + b_1s + b_\circ} \tag{22}$$

From (12 and 21), the controller gain is given by:

$$K_p^{mfc} = \frac{\left(3.4\omega_n^2 - \tau_{2\omega}\right)}{K_{tmpq}K_i^{\omega}} \tag{23}$$

The stability limit of the proportional gain K_p^{mfc} of the MFC can be determined by $\omega_r^{mfc}(s) = 0$ using Routh Hurwitz stability criterion. The selection of the limiting value of the K_p^{mfc} during parameter variation (rotor time constant and motor intertia) can be calculated from (24) and found from Fig. 5.

$$\omega_r^{mfc}(s) = b_4s^4 + b_3s^3 + b_2s^2 + b_1s + b_\circ$$
$$= \begin{bmatrix} s^4 + s^3(\tau_i + 1/\tau_m + K_{tmpq}K_d^{\omega}) + s^2(\tau_{2\omega} + K_{tmpq}K_i^{\omega}K_p^{mfc}) \\ + s(\tau_{1\omega} - K_{tmpq}K_i^{\omega} + K_{tmpq}K_i^{\omega}K_{PI}^{i}K_p^{mfc} + K_{tmpq}K_i^{\omega}K_i^{\omega}) \\ + K_{tmpq}K_i^{\omega}K_i^{\omega}K_{PI}^{i} = 0 \end{bmatrix} \tag{24}$$

3.2.2 MFC with PI-Controller (PI-MFC)

Similar to P-MFC, the closed loop transfer function shown in Fig. 4 is given by:

$$\frac{\omega_r(s)}{\omega_r^{mfc}(s)} = \frac{c_4s^4 + c_3s^3 + c_2s^2 + c_1s + c_\circ}{d_4s^4 + d_3s^3 + d_2s^2 + d_1s + d_\circ} \tag{25}$$

From (12 and 21), the controller gains are given by:

$$K_p^{mfc} = \frac{\left(3.4\omega_n^2 - \tau_{2\omega}\right)}{K_{tmpq}K_i^{\omega}} \tag{26}$$

$$K_i^{mfc} = \frac{\left(\omega_n^4 - K_{tmpq}K_i^{\omega}K_i^{\omega}K_{PI}^{i}\right)}{K_{tmpq}K_i^{\omega}K_{PI}^{i}} \tag{27}$$

Also, the stability limit of the MFC parameters, K_p^{mfc} and K_i^{mfc} can be obtained by setting $\omega_r^{mfc}(s) = 0$ and using the Routh Hurwitz stability criterion. The selection of the limiting value of controller gains under parameter variations (rotor time constant and motor intertia) can be calculated from (28) and found from Fig. (6).

$$\omega_r^{mfc}(s) = d_4s^4 + d_3s^3 + d_2s^2 + d_1s + d_\circ$$
$$= \begin{bmatrix} s^4 + s^3(\tau_i + 1/\tau_m + K_{tmpq}K_d^{\omega}) + s^2(\tau_{2\omega} + K_{tmpq}K_i^{\omega}K_p^{mfc}) \\ + s(\tau_{1\omega} - K_{tmpq}K_i^{\omega} + K_{PI}^{i}K_p^{mfc} + K_i^{\omega} + K_i^{mfc}) \\ + K_{tmpq}K_i^{\omega}K_{PI}^{i}(K_i^{\omega} + K_i^{mfc}) = 0 \end{bmatrix} \tag{28}$$

$\tau_{\circ\omega} = K_{tmpq}K_{PI}^{i}K_i^{\omega}$, $\tau_{1\omega} = (K_{iq}/\tau_m + K_{tmpq}K_{PI}^{i}K_p^{\omega} + K_{tmpq}K_i^{\omega})$,

$\tau_{2\omega} = (K_{iq} + \tau_i/\tau_m + K_{tmpq}K_p^{\omega} + K_{tmpq}K_{PI}^{i}K_d^{\omega})$,

$\tau_{3\omega} = (\tau_i + 1/\tau_m + K_{tmpq}K_d^{\omega})$, $K_{tmpq} = K_tK_mK_{pq}$,

$K_j = (P/2)/J$, $K_{pq} = K_{qde}K_p^{i}$, $\tau_m = J/\beta$, $K_{iq} = K_{qde}K_i^{i}$,

$\tau_{sr}^{'} = \tau_s^{'}\tau_r^{'}/(\tau_r^{'} + \tau_s^{'}(1-\sigma))$, $\tau_i = (1 + K_{pq}\tau_{sr}^{'})/\tau_{sr}^{'}$,

$K_{qde} = 1/\sigma L_s$, $K_{PI}^{i} = K_i^{i}/K_p^{i}$, $\tau_1 > \tau_2$, $\tau_2 = (K_p^{\omega}/K_i^{\omega})$,

$\overline{K} = \omega_n^4/K_{tmpq}K_i^{\omega}K_{PI}^{i}$, $a_4 = K_i^{\omega}$, $a_3 = \tau_{3\omega}K_i^{\omega}$,

$a_2 = K_i^{\omega}(\tau_{2\omega} + K_{tmpq}K_p^{mfc})$, $a_1 = K_i^{\omega}(\tau_{1\omega} + K_{tmpq}K_{PI}^{i}K_p^{mfc})$,

$a_\circ = \tau_{\circ\omega}K_i^{\omega}$, $b_4 = 1$, $b_3 = (\tau_i + 1/\tau_m + K_{tmpq}K_d^{\omega})$,

$$b_2 = (\tau_{2\omega} + K_{tmpq} K_i^{\omega} K_p^{mfc}),$$

$$b_1 = (\tau_{1\omega} - K_{tmpq} K_i^{\omega} + K_{tmpq} K_i^{\omega} K_{PI}^{i} K_p^{mfc} + K_{tmpq} K_i^{\omega} K_i^{\omega}),$$

$$b_0 = K_{tmpq} K_i^{\omega} K_i^{\omega} K_{PI}^{i},\ c_4 = K_i^{\omega},\ c_3 = \tau_{3\omega} K_i^{\omega},$$

$$c_2 = K_i^{\omega} (\tau_{2\omega} + K_{tmpq} K_p^{mfc}),$$

$$c_1 = K_i^{\omega} (\tau_{1\omega} + K_{tmpq} (K_{PI}^{i} K_p^{mfc} + K_i^{\omega} + K_i^{mfc})),$$

$$c_0 = K_i^{\omega} (\tau_{0\omega} + K_{PI}^{i} (K_i^{\omega} + K_i^{mfc})),\ d_4 = 1,$$

$$d_3 = (\tau_i + 1/\tau_m + K_{tmpq} K_d^{\omega}),$$

$$d_2 = (\tau_{2\omega} + K_{tmpq} K_i^{\omega} K_p^{mfc}),$$

$$d_1 = (\tau_{1\omega} - K_{tmpq} K_i^{\omega} + K_{PI}^{i} K_p^{mfc} + K_i^{\omega} + K_i^{mfc}),$$

$$d_0 = K_{tmpq} K_i^{\omega} K_{PI}^{i} (K_i^{\omega} + K_i^{mfc})$$

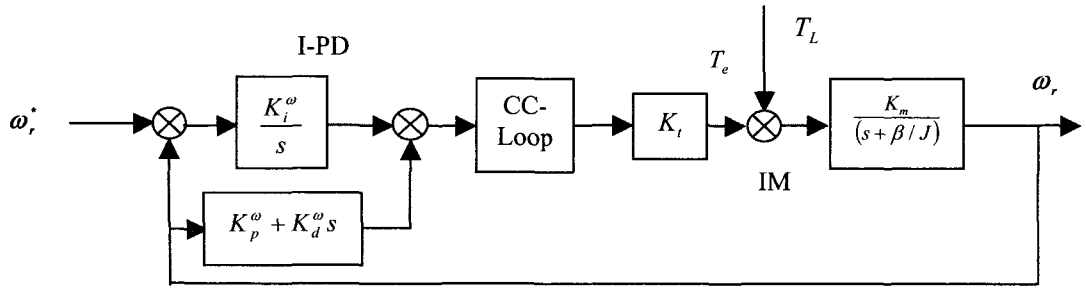

Fig. 2 The block diagram of induction machine speed control with an I-PD controller

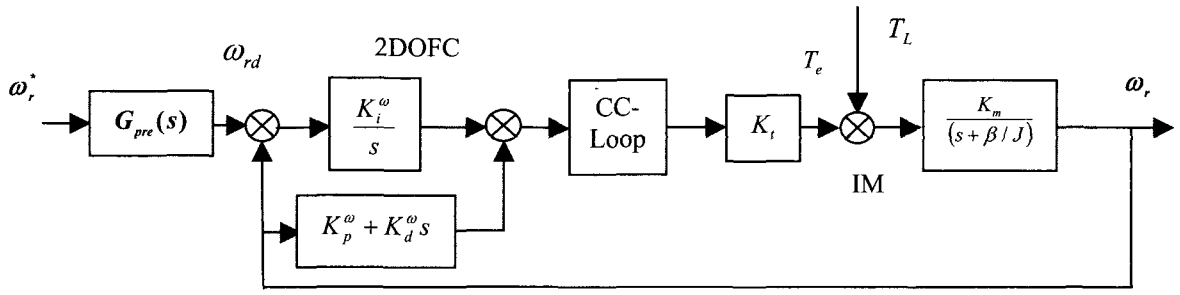

Fig. 3 The block diagram of the speed control with a 2DOF I-PD controller

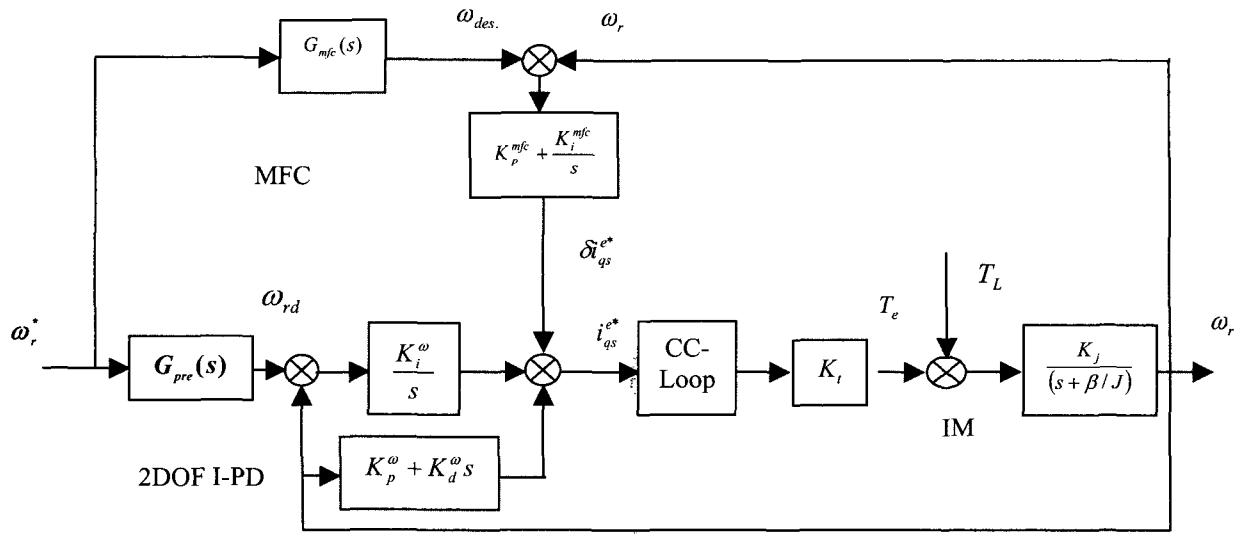

Fig. 4 The block diagram of the speed control with a 2DOF I-PD model following controller

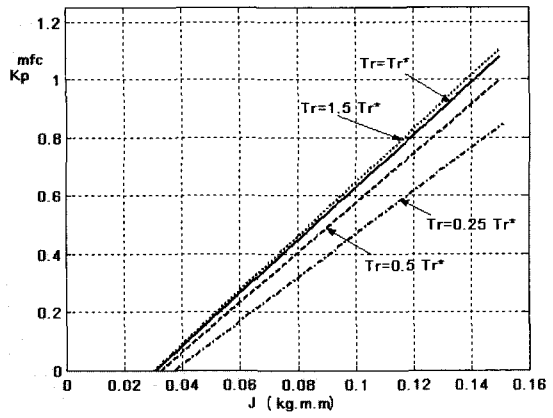

Fig. 5 The limiting values of K_p^{mfc} during under parameter variations

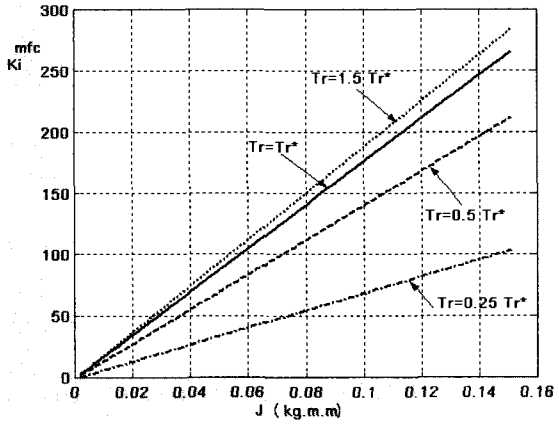

Fig. 6 The limiting values of K_i^{mfc} during under parameter variations

4. Simulation Results

The simulations are carried out for the induction motor drive system with the specifications listed in Table 1.

Table 1 Machine parameters

Type: three-phase induction motor
1.5 kW, 4 poles, 380 V/3.8 A, 50 Hz
$R_s = 6.29\,\Omega, R_r = 3.59\,\Omega$, $L_s = L_r = 480\,mH, L_m = 464\,mH$,
$J = 0.038\,\text{kg.m}^2$, $\beta = 0.008345$ N.m/rad/sec

This section presents the results of the simulations comparing a 2DOF I-PD with a MFC controller to a 2 DOF I-PD without a MFC controller. *d-q* axes current controllers and a speed controller are used to study the dynamic performance of the two drive systems under different operating conditions, including load changes. These simulations verify the feasibility of the proposed control scheme shown in Fig. 1.

The performance of the drive system with the proposed 2DOF I-PD and 2DOF I-PD MFC speed controllers are shown in Figs. 7-13 under an external load of 11.5 N.m with the machine parameters fixed at the nominal values. The simulation results of the 2DOF I-PD speed controller are shown in Fig. 7. The results include the command and actual *d-q* axes currents, command torque and actual torque and the speed responses. They clearly illustrate good performance in command tracking and load regulation. Also, Fig. 8 shows the simulation's results using a 2DOF I-PD MFC speed controller. These responses demonstrate the robust control performance and the rapid, accurate response of the reference model. The simulation results of the 2DOF I-PD and 2DOF I-PD MFC speed controllers, respectively are shown in Figs. 9-10. It is clear from Fig. 9 that there is an obvious model-following error with the 2DOF I-PD speed controller. However, a model-following error-driven adaptation signal is generated for the 2DOF I-PD MFC speed controller, which corrects the model-following control performance. The rotor speed responses for the 2DOF I-PD MFC speed controller are shown in Fig. 10. By augmenting the 2DOF I-PD controller with a MFC speed controller, command tracking and load regulation performance are improved as seen in Fig. 11. Its clear from this figure that the proposed 2DOF I-PD MFC speed controller provides a rapid and accurate response for the reference model within 0.5 sec. Also, the proposed controller quickly returns the speed within 1.5 sec under full load with a maximum decrease of 8 rad/sec, compared to the 2DOF I-PD speed controller which gives a slow response of about 1 sec and a large decrease in speed of about 30 rad/sec.

To investigate the effectiveness of the proposed hybrid speed controller, four cases with parameter variations in the rotor time constant, motor inertia and load torque disturbance are considered. The following possible ranges of parameter variations and external disturbances are considered.

Case 1: $\tau_r = \tau_r^*$, $J = J^*$, T_L=0-11.5 N.m

Case 2: $\tau_r = 1.5\ \tau_r^*, J = 5 \times J^*$, T_L=0-11.5 N.m

Case 3: $\tau_r = 0.5\ \tau_r^*, J = 5 \times J^*$, T_L=0-11.5 N.m

Case 4: $\tau_r = 0.25\ \tau_r^*$, $J = 5 \times J^*$, T_L=0-11.5 N.m

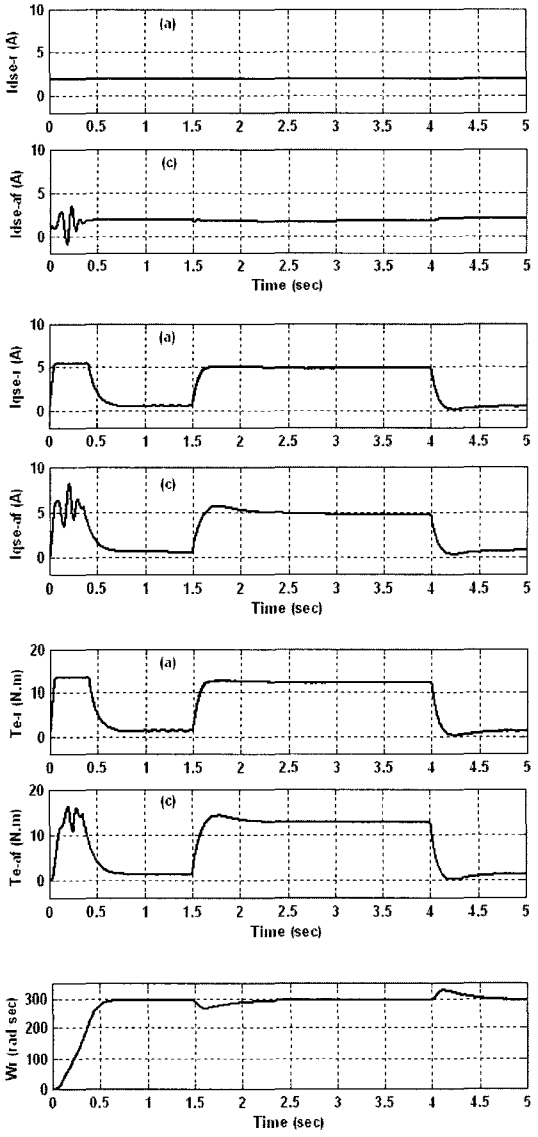

(a) reference (c) actual

Fig. 7 Step responses in speed reference and load disturbance with 2DOF I-PD speed controller

The speed response and the load regulation performance of the drive system with the 2DOF I-PD and 2DOF I-PD MFC speed controllers are shown in Figs. 12-13, respectively, under the conditions where the rotor time constant changes from 0.25 τ_r to 1.5 τ_r and the motor inertia constant changes from J to 5J. At t = 1.5 sec, an external load of 11.5 N.m is applied to the drive system and removed at t = 4 sec. Fig. 12 illustrates the speed tracking response and load regulation performance for the 2DOF I-PD speed controller with parameter variations. The speed response is significantly affected by variations in the machine parameters. Fig. 13 shows the speed tracking response and load regulation performance for the 2DOF I-PD MFC speed controller under machine parameter variations. In this case, the speed response is influenced less by the external load than the 2DOF I-PD speed controller.

5. Conclusion

This paper proposes a robust 2DOF I-PD MFC speed controller for an induction motor drive system under IFOC which guarantees robustenss in the presence of parameter variations. Quantitative design procedures for the 2DOF I-PD and 2DOF I-PD MFC controllers have been successfully developed in this paper. First, the I-PD speed controller was designed according to the prescribed command tracking specifications. The closed loop transfer function was chosen as the reference model. Next, the feed-forward controller was designed as a lead/lag compensator to improve the disturbance rejection characteristics of the drive system. Then, a model-following controller (MFC) was designed and added to the 2DOF I-PD speed controller to preserve the performance of the controller in spite of parameter variations and external disturbance. In designing the 2DOF I-PD MFC speed controller, the desired command-tracking specifications were defined in the reference model and the difference between the outputs of the reference model and the actual rotor speed was used to activate the MFC controller. It follows that the rotor speed tracking response can be regulated to closely follow the response of the reference model under a wide range of operating conditions. The performance of the drive system and the effectiveness of the proposed controllers have been demonstrated by a wide range of simulation results. Simulation results have shown that the proposed 2DOF I-

PD MFC speed controller grants accurate tracking and regulation characteristics in the face of motor parameter variations and external load disturbance. Therefore, it can be expected that the proposed control scheme can be applied to high performance applications.

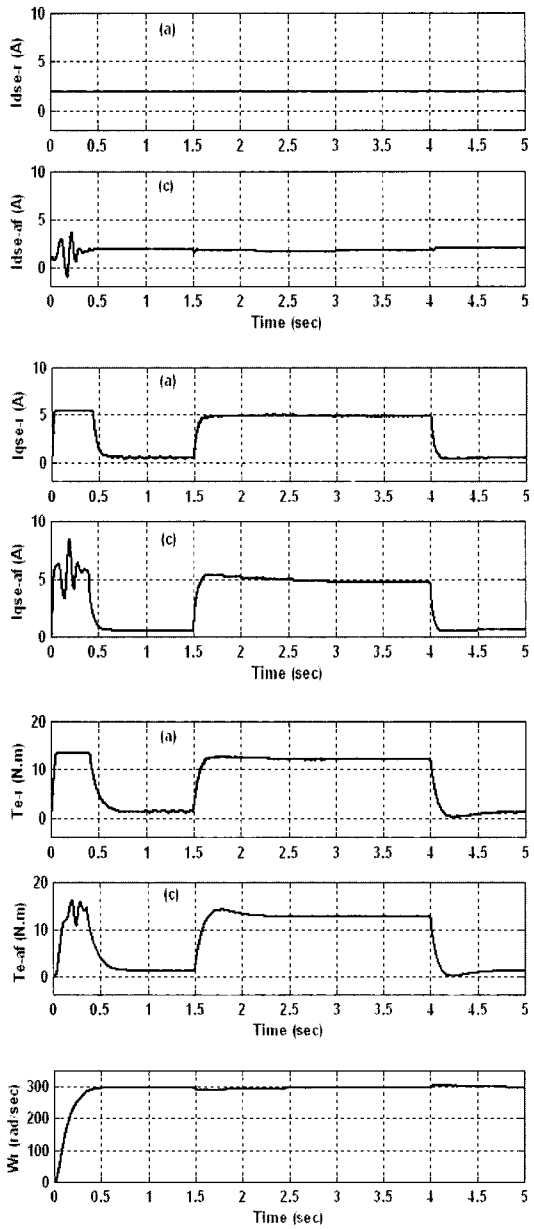

(a) reference (c) actual

Fig. 8 Step responses in speed reference and load disturbance using a 2DOF I-PD MFC speed controller

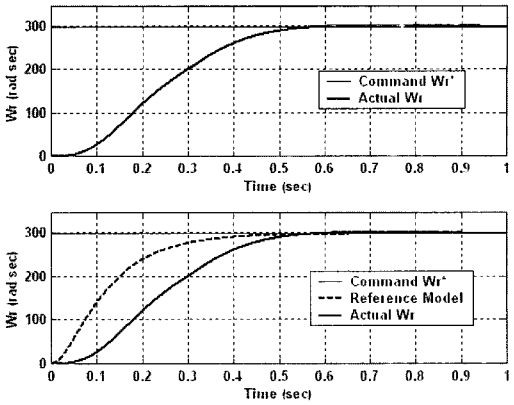

Fig. 9 The speed tracking response using the reference model and a 2DOF I-PD speed controller

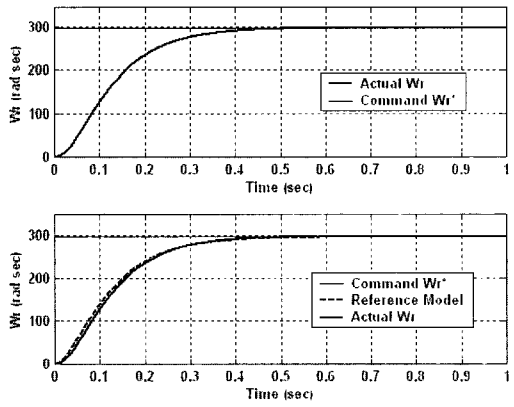

Fig. 10 The speed tracking response using the reference model and a 2DOF I-PD MFC speed controller

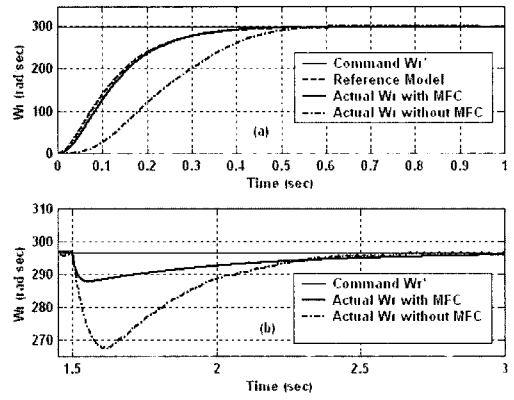

Fig. 11 Comparison between the speed tracking response and load regulation performance with and without a MFC

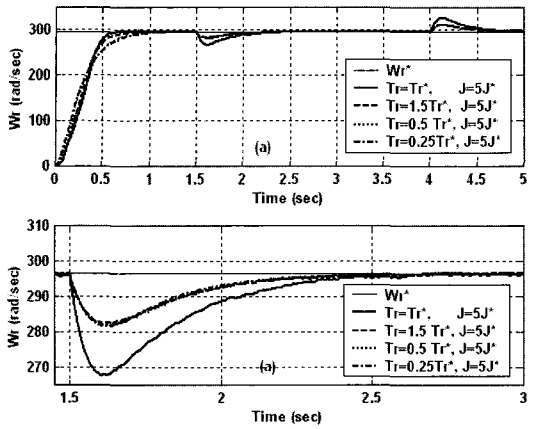

Fig. 12 The effect of parameter variations on a 2DOF I-PD speed controller

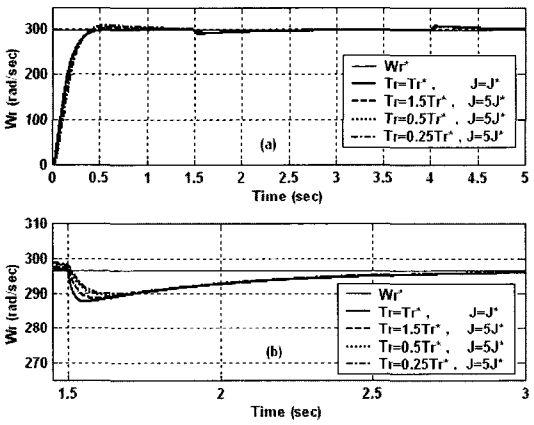

Fig. 13 The effect of parameter variations with on a 2DOF I-PD MFC speed controller

References

[1] B. K. Bose, Modern Power Electronics and AC Drives, Prentice Hall, Upper Saddle River, 2002.

[2] Peter Vas, Vector Control of AC Machines, Oxford: Clarendon Press, 1990.

[3] Ned Mohan, Advanced Electrric Drives: Analysis, control, and Modeling using Simulink, MNPERE Press, USA, 2001.

[4] Fayez F. M. El-Sousy, Faeka M.H. Khater and Farouk I. Ahmed, "Analysis and Design of Indirect Field Orientation Control for Induction Machine Drive System", Proceeding of the 38th SICE annual conference, SICE99, Iwate, Japan, July 28-30, pp. 901-908, 1999.

[5] K.B. Nordin., D.W. Novotny, and D. S.Zinger, "The influence of motor parameter deviations in feedforward field orientation drive systems", IEEE Trans. Ind. Appl., July/Aug., Vol. IA-21, No. 4, pp. 624-632, 1985.

[6] L. J. Garces, "Parameter adaptation for the speed controlled static ac drive with a squirrel cage induction motor", IEEE Trans. Ind. Appl., Mar./Apr., Vol. IA-16, No. 2, pp. 173-178, 1980.

[7] T. Matsuo T.A. and Lipo, "Rotor resistance identification in the field oriented control of a squirrel cage induction motor", IEEE Trans. Ind. Appl., May/July, Vol. IA-21, No. 3, pp. 624-632, 1985.

[8] R. Kirshnan and F.C. Doran, "Study of parameter sensitivity in high-performance inverter-fed induction motor drive system", IEEE Trans. Ind. Appl., May/July, Vol. IA-23, No. 4, pp. 623-635, 1992.

[9] C. M. Liaw, "Design of a two-degrees-of-freedom controller for motor drives", IEEE Trans. Automatic Control., Aug./Sept., Vol. AC-37, No. 4, pp. 1215-1220, 1992.

[10] C. M. Liaw and F.J. Lin, "A robust speed controller for induction motor drives", IEEE Trans. Ind. Elect., Aug./Sept., Vol. IE-41, No. 4, pp. 308-315, 1994.

[11] Fayez F. M. El-Sousy and Maged N. F. Nashed, "Robust Fuzzy Logic Current and Speed Controllers for Field-Oriented Induction Motor Drive", The Korean Institute of Power Electronics (KIPE), Journal of Power Electronics (JPE), Vol. 3, No. 2, pp. 115-123,. April, 2003.

[12] Fayez F. M. El-Sousy and M. M. Salem, "Simple Neuro-Controllers for Field Oriented Induction Motor Servo Drive System ", The Korean Institute of Power Electronics (KIPE), Journal of Power Electronics (JPE), Vol. 4, No. 1, pp. 28-38, January 2004.

[13] Fayez F. M. El-Sousy and M. M. Salem, "High Performance Simple Position Neuro-Controller for Field-Oriented Induction Motor Servo Drives" WSEAS Transactions on Systems, Issue 2, Vol. 3, pp. 941-950, April 2004.

[14] Fayez F. M. El-Sousy and Maged N. F. Nashed, "PID-Fuzzy Logic Position Tracking Controller for Detuned Field-Oriented Induction Motor Servo Drive", WSEAS Transactions on Systems, Issue 2, Vol. 3, pp. 707-713, April 2004.

[15] Fayez F. M. El-Sousy, "Design and Implementation of 2DOF I-PD Controller for Indirect Field Orientation Control Induction Machine Drive System", ISIE 2001 IEEE International Symposium on Industrial Electronics, Pusan, Korea, June 12-16, pp. 1112-1118, 2001.

[16] Matlab Simulink User Guide, The Math Work Inc., 1997

[17] C. M. Ong, Dynamic Simulation of Electric Machinery Using Matlab and Simulink. Printice Hall, 1998.

Fayez Fahim El-Sousy was born in Gahrbia Prefecture, Egypt in 1965. He received the B.Sc. degree in Electrical Power and Machines Engineering from Menoufia University, Egypt in 1988, the M.Ss. degree in Electrical Power and Machines Engineering from Cairo University, Egypt in 1994 and the Ph.D degree in Electrical Power and Machines Engineering from Cairo University, Egypt in 2000. Since 1990, he has been with the Department of Power Electronics and Energy Conversion at the Electronics Research Institute (ERI) where he is currently an Assistant Professor. His research interests are in the areas of modeling and control of ac machine drives, fuzzy control, optimal control, neural network control of electrical machines and power electronics. Dr. El-Sousy is currently a visiting researcher at Kyushu University, Graduate School of Information Science and Electrical Engineering, Yoshida Laboratory, Japan